Dalitz analysis section

Tom Latham
Anton Poluektov

The University of Warwick

1 July 2011

Physics on the B factories workshop
Annecy, 30 June – 1 July 2011

Section outline

- Introduction
  - Three-body decay phase space
  - Boundaries, kinematic constraints
  - Examples of usage
- Amplitude description
  - Dynamics: Isobar, K-matrix, non-resonant description
  - Angular dependence
- Experimental effects
  - Backgrounds, efficiency
  - Momentum resolution and cross-feed
- Tecnical details
  - Modifications of phase space: identical particles, square Dalitz plots.
  - Fitting: binned, unbinned, time-dependent, normalization
  - Fit fractions
- Model uncertainties
  - Esimation
  - Model-independent analysis
  - Model-independent PWA

Section status

- Introduction
  - Three-body decay phase space
  - Boundaries, kinematic constraints
  - Examples of usage

  [Gianluca Cavoto]

  Confirmed OK: no feedback yet
- Amplitude description
  - Isobar, non-resonant description, Angular dependence

    [Alexey Garmash]

    No response yet: probably not available
  - K-matrix

    [Fernando Martinez-Vidal]

    Draft in SVN

Section status

- Experimental effects
  - Backgrounds, efficiency
    [Tom Latham] Working, no text yet
  - Momentum resolution and cross-feed
    [Matt Graham] Draft exists, not in SVN
- Tecnical details
  - Modifications of phase space: identical particles, square Dalitz plots.
    [Eli Ben-Haim, Matt Graham] Draft in SVN
  - Time-dependent fits
    [Matt Graham] Draft exists, not in SVN
  - Fitting: binned, unbinned, normalization
    [Not assigned: Tom & Anton?]
  - Fit fractions
    [Tom Latham] Working, no text yet
- Model dependence
  [Anton]
  Parts of text (shared with ϕ_3 section)

Section in SVN

Contents

Chapter 10
Dalitz analysis

Editors:
Thomas Latham (BABAR)
Anton Poluektov (Belle)

10.1 Introduction

10.1.1 Three-body decay phase space

10.1.2 Boundaries, kinematic constraints

10.1.3 Examples of usage

10.2 Amplitude description

Non-leptonic B and D decays proceed predominantly through resonant two-body decays and this is the observed pattern ?. For three-body decays of a spin-0 particle (D or B meson) to all pseudo-scalar final state particles abc, the baseline model adopted to describe the decay amplitude $\mathcal{A}(m^2_{ab}, m^2_{bc})$ consists of a coherent sum of two-body amplitudes (subscript r) and a "non-resonant" (subscript NR) contribution ?,

$$\mathcal{A}_D(\mathbf{m}) = \sum_r a_r e^{i\phi_r} \mathcal{A}_r(\mathbf{m}) + a_{\rm NR} e^{i\phi_{\rm NR}}. \quad (1)$$

The parameters a_r ($a_{\rm NR}$) and ϕ_r ($\phi_{\rm NR}$) are the magnitude and phase of the amplitude for component r (NR). The function $\mathcal{A}_r = F_D \times F_r \times T_r \times W_r$ is a Lorentz-invariant expression that describes the dynamic properties of the B or D meson decaying into the multibody final state through an intermediate resonance r, as a function of position in the Dalitz plane $\mathbf{m} \equiv (m^2_{ab}, m^2_{bc})$. Here, F_D (F_r) is the Blatt-Weisskopf centrifugal barrier factor for the D or B meson (resonance) decay vertex ? with radius R, T_r is the resonance propagator, and W_r describes the angular distribution in the decay. This approach is usually referred to as isobar model.

10.2.1 Dynamics

The resonance propagator T_r is usually described using a relativistic Breit-Wigner (BW) parameterization with mass-dependent width ?, except for the wide $\rho(770)^0$ and $\rho(1450)^0$ resonances where a Gounaris-Sakurai (GS) functional form ? provides a better description. Mass and width values are in general taken from world averages ?, unless in some particular cases. The P- and D-waves of the decay amplitude are described using a certain number of BW or GS propagators, the actual number depending on the specific decay, while the S-waves descriptions are more complex and different alternatives haven been adopted.

The complex $\pi\pi$ S-wave dynamics, e.g in the $D^0 \to K^0_S\pi^+\pi^-$ reaction ?, with the presence of several broad and overlapping scalar resonances, is more adequately described through the use of a K-matrix formalism ? with the P-vector approximation ?. This approach offers a direct way of imposing the unitarity constraint of the scattering matrix, not guaranteed in the case of the isobar model. The Dalitz plot amplitude $\mathcal{A}(\mathbf{m})$ given by Eq. (1) is then modified as

$$\mathcal{A}_D(\mathbf{m}) = F_1(s) + \sum_{r \neq (\pi\pi)_{L=0}} a_r e^{i\phi_r} \mathcal{A}_r(\mathbf{m}) + a_{\rm NR} e^{i\phi_{\rm NR}}, \quad (2)$$

where $F_1(s)$ is the contribution of $\pi\pi$ S-wave states written in terms of the K-matrix formalism,

$$F_u(s) = \sum_l \left[I - iK(s)\rho(s)\right]^{-1}_{ul} P_v(s). \quad (3)$$

Here, $s = m^2_0$ is the squared invariant mass of the $\pi^+\pi^-$ system, I is the identity matrix, K is the matrix describing the S-wave scattering process, ρ is the phase-space matrix, and P is the initial production vector (P-vector). The index u (and similarly v) represents the $u^{\rm th}$ channel ($1 = \pi\pi$, $2 = K\overline{K}$, $3 = \pi\pi\pi\pi$, $4 = \eta\eta$, $5 = \eta\eta'$). In this framework, the production process can be viewed as the initial preparation of several states, which are then propagated by the $\left[I - iK(s)\rho(s)\right]^{-1}$ term into the final one. The propagator can be described using scattering data, provided that the two-body system in the final state is isolated and does not interact with the rest of the final state in the production process. The P-vector has to be determined from the data themselves since it depends on the production mechanism. Only the F_1 amplitude appears in Eq. (2) since we are describing the $\pi\pi$ channel.

The parameterizations adopted by *BABAR* for K, ρ, and P in Eq. (3) are the same as used by previous experiments ???. For the K matrix it is

$$K_{uv}(s) = \left(\sum_\alpha \frac{g^\alpha_u g^\alpha_v}{m^2_\alpha - s} + f^{\rm scatt}_{uv} \frac{1 - s^{\rm scatt}_0}{s - s^{\rm scatt}_0}\right) f_{A0}(s), \quad (4)$$

where g^α_u is the coupling constant of the K-matrix pole m_α to the $u^{\rm th}$ channel. The parameters $f^{\rm scatt}_{uv}$ and $s^{\rm scatt}_0$ describe the slowly-varying part of the K-matrix. The factor

$$f_{A0}(s) = \frac{1 - s_{A0}}{s - s_{A0}} \left(s - s_A \frac{m^2_\pi}{2}\right), \quad (5)$$

suppresses the false kinematical singularity at $s = 0$ in the physical region near the $\pi\pi$ threshold (the Adler zero ?). The parameter values used in this analysis are listed in Table 1, and are obtained from a global analysis of the available $\pi\pi$ scattering data from threshold up to 1900 MeV/c^2 ?. The parameters $f^{\rm scatt}_{uv}$, for $u \neq 1$, are all set to zero since they are not related to the $\pi\pi$ scattering process. Similarly, for the P vector we have

$$P_v(s) = \sum_\alpha \frac{\beta_\alpha g^\alpha_v}{m^2_\alpha - s} + f^{\rm prod}_{1v} \frac{1 - s^{\rm prod}_0}{s - s^{\rm prod}_0}. \quad (6)$$

Note that the P-vector has the same poles as the K-matrix, otherwise the F_1 vector would vanish (diverge) at the K-matrix (P-vector) poles. The parameters β_α, $f^{\rm prod}_{1v}$ and $s^{\rm prod}_0$ of the initial P-vector depend on the production mechanism and cannot extrapolated from scattering data, thus these have to be determined directly from the D or B meson decay data sample.

Table 1. K-matrix parameters from a global analysis of the available $\pi\pi$ scattering data from threshold up to 1900 MeV/c^2 ?. Masses and coupling constants are given in GeV/c^2.

m_α	$g^\alpha_{\pi^+\pi^-}$	$g^\alpha_{K\overline{K}}$	$g^\alpha_{4\pi}$	$g^\alpha_{\eta\eta}$	$g^\alpha_{\eta\eta'}$
0.65100	0.22889	−0.55377	0.00000	−0.39899	−0.34639
1.20360	0.94128	0.55095	0.00000	0.39065	0.31503
1.55817	0.36856	0.23888	0.55639	0.18340	0.18681
1.21000	0.33650	0.40907	0.85679	0.19906	−0.00984
1.82206	0.18171	−0.17558	−0.79658	−0.00355	0.22[illegible]

$s^{\rm scatt}_0$	$f^{\rm scatt}_{11}$	$f^{\rm scatt}_{12}$	$f^{\rm scatt}_{14}$	$f^{\rm scatt}_{15}$
−3.92637	0.23399	0.15044	−0.20545	0.32825	0.35412

s_{A0}	s_A
−0.15	1

The $K\pi$ S-wave contribution to Eq. (2) consists either of a $K^*_0(1430)^-$ BW that neglects possible non-resonant contribution or a $K^*_0(1430)^-$ BW together with an effective range non-resonant component with a phase shift derived scattering data ?,

$$\mathcal{A}_{K\pi\ L=0}(\mathbf{m}) = F \sin\delta_F e^{i\delta_F} + R \sin\delta_R e^{i\delta_R} e^{i2\delta_F}, \quad (7)$$

with

$$\delta_R = \phi_R + \tan^{-1}\left[\frac{M\Gamma(m^2_{K\pi})}{M^2 - m^2_{K\pi}}\right],$$
$$\delta_F = \phi_F + \cot^{-1}\left[\frac{1}{aq} + \frac{rq}{2}\right]. \quad (8)$$

The parameters a and r play the role of a scattering length and effective interaction length, respectively, F (ϕ_F) and R (ϕ_R) are the amplitudes (phases) for the non-resonant and resonant terms, and q is the momentum of the spectator particle in the $K\pi$ system rest frame. Note that the phases δ_F and δ_R depend on $m^2_{K\pi}$. M and $\Gamma(m^2_{K\pi})$ are

Section in SVN

the mass and running width of the resonant term. This parameterization corresponds in fact to a K-matrix approach describing a rapid phase shift coming from the resonant term and a slow rising phase shift governed by the non-resonant term, with relative strengths R and F ?. The parameters M, Γ, F, ϕ_F, R, ϕ_R, a and r are determined from our fit to the tagged D^0 sample, along with the other parameters of the model. Other recent experimental efforts to improve the description of the $K\pi$ S-wave using K-matrix and model independent parameterizations from high-statistics samples of $D^+ \to K^-\pi^+\pi^+$ decays are described in Ref. ?.

The fifth P-vector channel and pole have also been excluded since the $\eta\eta'$ threshold and the pole mass m_5 are both far beyond our $\pi\pi$ kinematic range, and thus there is little sensitivity to the associated parameters, $f_{15}^{\rm prod}$ and β_5, respectively.

The amplitudes are measured with respect to $D^0 \to K_S^0\rho(770)^0$ which gives the second largest contribution.

10.2.2 Angular dependence

The angular dependence W_r is described using either Zemach tensors ?? where transversality is enforced or the helicity formalism ??? when we allow for a longitudinal component in the resonance propagator (see Ref. ? for a comprehensive summary).

10.2.3 Non-resonant description

10.3 Experimental effects

10.3.1 Backgrounds

10.3.2 Efficiency

10.3.3 Momentum resolution and self cross feed

10.4 Technical details

10.4.1 Modifications of phase space

10.4.1.1 Identical particles in the final state

In case of identical particles in the final state, the phase space must be symmetrized.

10.4.1.2 The square Dalitz plot

A common feature of Dalitz plot analyses of B-meson decay to charmless final state is that both the signal events and the combinatorial $e^+e^- \to q\bar{q}$ ($q = u, d, s, c$) continuum background events populate the kinematic boundaries of the Dalitz plot. This is due to the low final state masses compared with the B mass. Large variations occurring in small areas of the Dalitz plot are difficult to describe in detail, and as a result, the typical Dalitz plot representation may be inconvenient when one wants to use empirical reference shapes in a maximum-likelihood fit. The boundaries of the Dalitz plot are particularly important since it is here that the interference between light meson resonances and hence the ability to determine the strong phases occurs. A solution that was adopted by some analyses is to apply a transformation to the kinematic variables that maps the Dalitz plot into a rectangle: the *Square Dalitz plot* (SDP). Such a transformation avoids the curved edge of bins on the boundary, which simplifies the use of non-parametric PDFs (histograms) to model the distribution of events over the Dalitz plot. Moreover, the transformation is required to expand the regions of interference to generally ease parameterization; for instance, equal size bins cover this region in more detail.

A common definition of the SDP is used, for example, in the *BABAR* $B^0 \to \pi^+\pi^-\pi^0$ analysis [XXX REF], where the SDP is obtained by the transformation:

$$ds_+\, ds_- \longrightarrow |\det J|\, dm'\, d\theta'. \qquad (9)$$

The variable s_+ (s_-) is the square invariant mass of the π^+ (π^-) and the π^0. The new coordinates are

$$m' \equiv \frac{1}{\pi}\arccos\left(2\frac{m_0 - m_0^{\rm min}}{m_0^{\rm max} - m_0^{\rm min}} - 1\right), \quad \theta' \equiv \frac{1}{\pi}\theta_0, \quad (10)$$

where $m_0 = \sqrt{s_0}$ is the invariant mass of the charged particles, $m_0^{\rm max} = m_{B^0} - m_{\pi^0}$ and $m_0^{\rm min} = 2m_{\pi^+}$ are the kinematic limits of m_0, θ_0 is the helicity angle of the ρ^0 resonance, which decays to the two charged pions, and J is the Jacobian of the transformation. Both new variables range between 0 and 1. The determinant of the Jacobian is given by

$$|\det J| \;=\; 4\,|\mathbf{p}_+^*||\mathbf{p}_0^*|\, m_0 \cdot \frac{\partial m_0}{\partial m'} \cdot \frac{\partial \cos\theta_0}{\partial \theta'}\,, \qquad (11)$$

where $|\mathbf{p}_+^*| = \sqrt{E_+^{*2} - m_{\pi^+}^2}$ and $|\mathbf{p}_0^*| = \sqrt{E_0^{*2} - m_{\pi^0}^2}$, and where E_+^* (E_0^*) is the energy of the π^+ (π^0) defined in the $\pi^+\pi^-$ rest frame. Figure 1 shows the determinant of the Jacobian as a function of the SDP parameters m' and θ'. If the events in the nominal Dalitz plot were distributed according to a uniform (non-resonant) three-body phases space, their distribution in the SDP would match the plot of $|\det J|$.

The effect of the transformation (9) is illustrated in Fig. 2, which displays the nominal and square Dalitz plots for simulated signal events generated with Monte Carlo. The benefits of the SDP that are explained above are clearly visible in this figure. This simulation does not take into account any detector effects and corresponds to a particular choice of the decay amplitudes for which destructive interferences occur where the ρ resonances overlap. To simplify the comparison, hatched areas showing the interference regions between ρ bands and dashed isocontours $\sqrt{s_{+,-,0}} = 1.5$ GeV/c^2 have been superimposed on both Dalitz plots.

Another transformation was used in the *BABAR* amplitude analysis of $B^0 \to K_S^0K_S^0K_S^0$ decays [XXX REF]. In this particular case, due to the symmetrization of phase space, the above transformation results in curved boundaries. On the other hand, mapping the invariant masses to the plane defined by two helicity angles results in a rectangle.

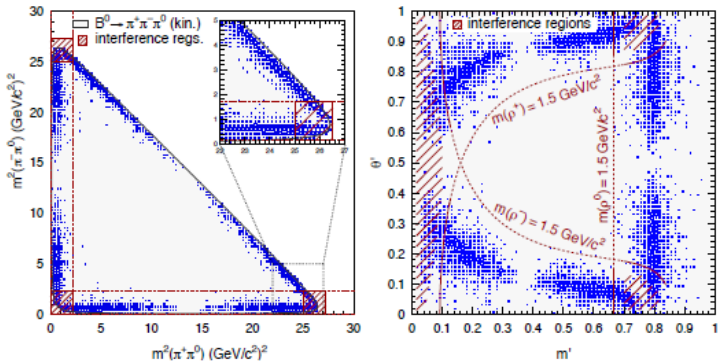

Fig. 2. Nominal (left) and square (right) Dalitz plots for Monte-Carlo generated $B^0 \to \pi^+\pi^-\pi^0$ decays. Comparing the two Dalitz plots shows that the transformation (9) indeed homogenizes the distribution of events, which are no longer near the plot boundaries but rather cover a larger fraction of the physical region. The decays have been simulated without any detector effect and the amplitudes A^+, A^- and A^0 have all been chosen equal to 1 in order to have destructive interferences where the ρ bands overlap. The main overlap regions between the ρ bands are indicated by the hatched areas. Dashed lines in both plots correspond to $\sqrt{s_{+,-,0}} = 1.5$ GeV/c^2; the central region of the Dalitz plot (defined by requiring that all 3 two-body invariant masses exceed this threshold) contains few signal events.

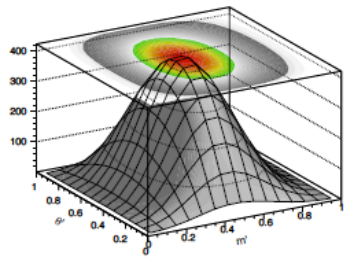

Fig. 1. Jacobian determinant (11) of the transformation (9) defining the square Dalitz plot (SDP). Such a distribution would be obtained in the SDP if events were uniformly distributed over the nominal Dalitz plot.

10.4.2 Fitting

10.4.3 Fit fractions

10.5 Model uncertainties

10.5.1 Estimation of model uncertainties

10.5.2 Model independent analysis

10.5.3 Model independent partial wave analysis

Conclusion

- Section only starts to take shape. Thanks to Eli, Matt and Fernando.
- Important parts are still missing:
  - Introduction
  - Isobar model, angular terms
- Still many cut-and-pastes in existing text.
- Everyone (obviously) extremely busy, communication has been difficult. Hopefully this will change as we have something to discuss.
- Not much contribution from Belle colleagues. Expect at least proofreading and comments (Alex Bondar, Alex Kuzmin, Alexey Garmash, Roman Mizuk).